Available online at www.sciencedirect.com

SCIENCE DIRECT

Developmental Biology 288 (2005) 434 – 447

DEVELOPMENTAL BIOLOGY

www.elsevier.com/locate/ydbio

Noelins modulate the timing of neuronal differentiation during development

Tanya A. Moreno [1], Marianne Bronner-Fraser *

Division of Biology, 139-74, California Institute of Technology, Pasadena, CA 91125, USA

Received for publication 3 August 2005, revised 9 September 2005, accepted 21 September 2005
Available online 14 November 2005

Abstract

Noelins comprise a family of extracellular proteins with proposed roles in neural and neural crest development. Here, we show that a previously uncharacterized family member, *Noelin-4*, functions to maintain neural precursors in an undifferentiated state and biases ectoderm toward a neural fate. We show that *Noelin-4* is induced by the neurogenic genes *X-ngnr-1* and *XNeuroD*. Over-expression of *Noelin-4* causes expansion of the neural plate at the expense of neural crest and epidermis. Although there is an apparent increase in the neural precursor pool, no increase was noted in differentiated neurons. Later, derivatives such as the neural tube and retina appear enlarged. We show biochemically that Noelin-4 protein is glycosylated and secreted and that it interacts with Noelin-1, an isoform previously found to promote differentiation in neuralized animal caps. Accordingly, the neural precursor expansion activity of *Noelin-4* is reversed by co-expression of *Noelin-1*. Our finding that *Noelin* isoforms can bind to and antagonize one another suggests that interacting *Noelin* isoforms may play a role in regulating timing of differentiation.

Keywords: Noelin-4; Noelin-1; Neurogenesis; Xenopus; Neural competence; Neural differentiation

Introduction

Neural development is a complex process that requires the activities of many opposing and cooperative gene networks and signaling pathways. In *Xenopus*, neural development begins during gastrulation when the dorsal mesoderm signals the overlying ectoderm to become neural (Chang and Hemmati-Brivanlou, 1998; Harland, 2000; Sasai and De Robertis, 1997; Weinstein and Hemmati-Brivanlou, 1999). First, a broad neural domain is established, characterized by expression of early response genes (Turner and Weintraub, 1994; Ferreiro et al., 1994; Kroll et al., 1998; Mizuseki et al., 1998a,b). Subsequently, neurogenesis is activated by a cascade of bHLH transcription factors, typified by the proneural and neurogenic genes *X-ngnr-1* and *XNeuroD* (Lee et al., 1995b; Ma et al., 1996), that determine which cells give rise to neurons within the field of cells with neural potential. Later-expressed factors influence specification and differentiation of neuronal subtypes. Many transcriptional regulators of these events have been characterized, but less is known about downstream components that mediate the process of neuronal differentiation.

Noelins are a family of secreted glycoproteins that have been implicated in both neural crest development and neurogenesis (Barembaum et al., 2000; Kulkarni et al., 2000). Four different *Noelin* isoforms are formed by differential promoter usage and alternative splicing (Danielson et al., 1994; see Fig. 1A): *Noelin-1* (BMZ), *Noelin-2* (AMZ), *Noelin-3* (BMY) and *Noelin-4* (AMY) from the five available exons, A, B, M, Y and Z (Barembaum et al., 2000; Danielson et al., 1994). These genes are part of a larger family of proteins containing an "olfactomedin domain," although *Noelin-3* and *-4* lack the exon that encodes this domain. The expression patterns of some of the *Noelin* isoforms have been described in mouse, rat, *Xenopus* and chick (Barembaum et al., 2000; Kondo et al., 2000; Moreno and Bronner-Fraser, 2001, 2002; Nagano et al., 1998, 2000). In early development, *Noelins* are expressed in the neural plate of chick and mouse; later, they resolve to the neural folds and migrating neural crest cells. In contrast, *Xenopus Noelin-1* is expressed after neural tube closure, and only in postmitotic neuronal cells. Postnatally, *Noelins* are expressed in the cortex of mouse brain (Nagano et al., 1998). Some functional studies have been undertaken to

* Corresponding author. Fax: +1 626 395 7717.
E-mail address: mbronner@caltech.edu (M. Bronner-Fraser).
[1] Present address: The Salk Institute, 10010 N. Torrey Pines Rd., La Jolla, CA 92037, USA.

0012-1606/$ - see front matter © 2005 Elsevier Inc. All rights reserved.
doi:10.1016/j.ydbio.2005.09.050

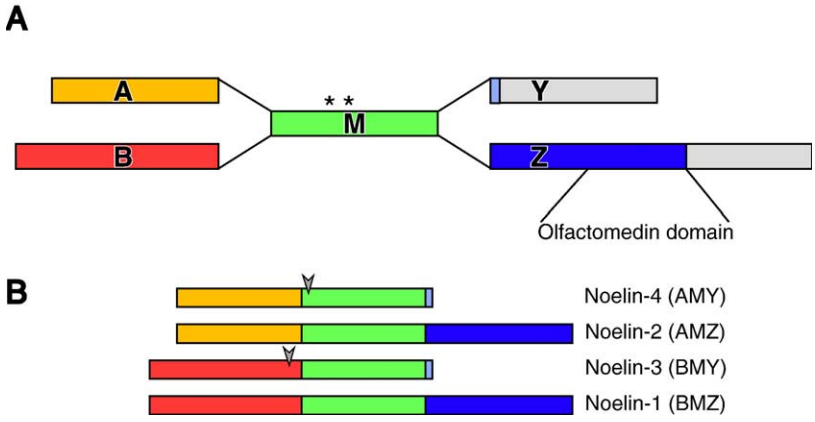

Fig. 1. Schematic diagram of *Noelin* isoform exon composition. (A) Noelins are made by differential promoter usage and alternative splicing. Exon structure was first elucidated in the rat by Danielson et al. (1994). The olfactomedin domain is indicated, as well as the location of the two cysteine residues conserved in all Noelins and homologous to cysteines in Olfactomedin that are responsible for disulfide bonding in multimerization (asterisks in M region). (B) Noelin exon terminology used in this work is shown, with predicted signal peptide cleavage sites indicated with arrowheads.

elucidate the role of these proteins during development. In chick, *Noelin-1* was shown to increase the competence of the neural tube to produce neural crest cells, while in *Xenopus*, *Noelin-1* promotes neuronal differentiation (Barembaum et al., 2000; Moreno and Bronner-Fraser, 2001). Although the function of *Noelin-1* has been characterized in these species, nothing is known about the function of *Noelin-4*.

In the present study, we explore the role of *Noelin-4* in *Xenopus* development and provide evidence for a unique function as a factor that maintains neural precursors in an undifferentiated state. Embryos injected with *Noelin-4* mRNA exhibit enlargement of neural precursor territories and later have enlarged retinas and ectopic neural structures resembling ganglia, otic vesicles and cement glands. This expansion of neural plate occurs apparently at the expense of neural crest and epidermis. Strikingly, the neural-expansion promoting activity of *Noelin-4* is reversed by co-expression of *Noelin-1*, to which it binds in co-immunoprecipitation assays. The overlapping expression pattern of *Noelin* isoforms, together with the biochemical and functional interactions of the Noelin-1 and -4 proteins, suggest a role for competitive Noelin interactions in regulating the timing of differentiation in the cells in which they are expressed.

Materials and methods

Library screening and cDNA isolation

A stage 28 phage cDNA library in Lambda ZapII made from head tissues was kindly provided by Dr. R. Harland (Hemmati-Brivanlou et al., 1991). Full-length clones of *Noelin-1*, *-2* and *-4* were obtained after low-stringency screening using chick *Noelin-1* as a probe. Sequences were compiled and edited using the DNAStar programs. Sequences comparisons were performed using BLAST (Altschul et al., 1990). Signal peptide prediction was done by a computer modeling method on the server http://www.cbs.dtu.dk/services/signalP (Nielsen et al., 1997).

Noelin-3 (encoded by exons BMY) was assembled from existing clones of *Noelin-1*. The B and M exons were amplified by PCR with the following oligos: upstream: 5′-CCA TCG ATC CAA GCA AAC ATG TCT GTG CC-3′, and downstream: 5′-AGG CAG TTT AAG GGC TGA ATT CCG-3′, these were cloned into pCS2+ (Rupp et al., 1994; Turner and Weintraub, 1994). The downstream oligo is complementary to the last 12 bases of the M exon, with an added glycine residue and stop codon (Y exon sequences).

Xenopus laevis embryo and oocyte manipulations

Xenopus embryos were obtained by in vitro fertilization using eggs from pigmented and albino females and testis from pigmented males, according to established methods (Sive et al., 2000). Embryos were staged according to the normal tables of (Nieuwkoop and Faber, 1967).

Animal caps were manually isolated from stage 8 to 9 blastulae and cultured in 3/4 × NAM (Slack and Forman, 1980) until siblings reached the stage indicated, when they were processed for RT-PCR.

Stage VI oocytes were manually defolliculated in OR2 and allowed to recover for one day before injection.

Microinjections

For oocytes: capped messenger RNA was transcribed in vitro (Sive et al., 2000) and up to 2 ng was injected per oocyte in a volume of up to 20 nl. Injected oocytes were cultured in OR2 medium supplemented with 1 mg/ml of BSA (Sigma), Gentamycin and 10 μCi of [^{35}S]-methionine (Express Protein Labeling Mix, NEN) in a total volume of 200 μl. Injected oocytes were cultured for 24 h. All samples were run in duplicate or triplicate for each experiment.

For embryos: capped messenger mRNA was transcribed as above, or by using the mMessage mMachine SP6 kit (Ambion). Varying concentrations were injected in volumes ranging from 5 to 10 nl at the two-cell stage, into both blastomeres for animal cap experiments, into one cell of two for whole embryo experiments, or 5 nl into 32-cell-stage blastomeres. *X-ngnr-1* was injected at 100 pg per embryo; *XNeuroD* was injected at 500 pg per embryo, *noggin* at 100 pg per embryo. *Noelin* isoforms were injected at a range from 50 pg to 1.5 ng as indicated in the text.

Embryos injected with *lac*Z were stained for β-galactosidase activity with X-Gal (Roche) or Magenta Gal (Biosynth).

Immunoprecipitations and Western blots

Oocyte and supernatant fractions were collected from duplicate samples containing 5 oocytes injected with the indicated mRNAs and cultured for 24 h. In vitro-translated protein was synthesized using the same mRNAs in Nuclease-treated Rabbit Reticulocyte Lysate (Promega) according to the manufacturer's instructions. Anti-*myc* antibody (mouse monoclonal antibody 9E10, Santa Cruz Biotechnology) was used at 1:500. Anti-*flag* M2 antibody (mouse monoclonal, Sigma) was used at 10 μg/ml. Samples were incubated with Protein A Sepharose (Sigma) to immunoprecipitate the antibody-bound proteins. Samples were run out on 14% SDS-PAGE gels

and analyzed on a Molecular Dynamics PhosphoImager. Western blots were performed using Enhanced Chemiluminescence (ECL, Pharmacia). Enzymatic deglycosylation was performed according to manufacturer's instructions (PNGase F, NEB).

In situ hybridization and immunohistochemistry

In situ hybridization was performed as described (Knecht et al., 1995). For immunohistochemistry, anti-phospho-histone H3 (rabbit IgG, Upstate Technologies) was diluted to 1:200. The antibody was detected with HRP-conjugated goat anti-rabbit IgG (Molecular Probes) at 1:400. For sectioning, embryos were embedded in Paraplast Plus wax and sectioned on a Leitz microtome at 10 μm. Sectioned whole mount in situs were counterstained in Light Green SF (Sigma). For TUNEL staining, embryos were incubated with 0.5 μM digoxygenin-labeled dUTP (Roche) and 150 U/ml Terminal deoxynucleotidyltransferase (Invitrogen) in 1× TdT buffer overnight at room temperature, stopped in PBS + 1 mM EDTA at 65°C, followed by washes in PBS and detection as for in situ hybridization.

RT-PCR analysis

RT-PCR analysis was as described (Moreno and Bronner-Fraser, 2001) on pools of total RNA from 2 embryos or 10 animal caps. First strand synthesis was performed with Superscript III Reverse Transcriptase (Life Technologies) with random hexamers (Life Technologies) according to manufacturer's instructions. Primers were as described in (Moreno and Bronner-Fraser, 2001) or below. One third of each PCR reaction was run on a 5% polyacrylamide gel and analyzed autoradiographically and on the PhosphorImager. Noelin isoform PCR primer pairs used were: A+Y, A+Z, B+Y, B+Z; each product approx. 330 nt, 30 cycles. *Noelin* A: 5′-GCA AGC TGA TGA GTC TCT TC-3′; *Noelin* B: 5′-GGA ACC TTG GAT AGG AGC-3′; *Noelin* Y: 5′-TGC CTC TTC AGT CTT TGC-3′; *Noelin* Z: 5′-CAA CAC TGG TAT CAG AGG-3′.

Results

Noelin-4 sequence and structure

Noelin isoforms include four splice variants assembled by differential promoter usage and alternative splicing. *Xenopus Noelin-4* contains the A, M, and Y exons, and is the smallest of the four *Noelin* splice variants (Fig. 1). The longest open reading frame from the first start codon (381 bp) encodes a predicted 126 amino acid (aa) protein with a molecular weight of approximately 14.7 kilodaltons (kDa). *Xenopus Noelin-4* is 89–92% identical at the nucleotide level to previously isolated rat (GenBank accession number I73636), mouse (pancortin-4, BAA28764), and human (JC5272) orthologues.

Noelin-4 has several recognizable sequence features including one N-linked glycosylation site and two potential hyaluronate binding sites. Noelin-4 also contains two cysteine residues that are conserved in all Noelin isoforms (Fig. 1A, asterisks) and that are spatially homologous to two cysteine residues in olfactomedin. These are thought to be responsible for intermolecular disulfide bonding in that protein (Yokoe and Anholt, 1993). Although Noelin-4 is slightly related to olfactomedin, the founding member of the olfactomedin domain family (Kulkarni et al., 2000; Snyder et al., 1991), it lacks the Z exon found in Noelin-1 and -2 that contains the olfacotmedin domain itself (Figs. 1A, B). As with Noelin-1 and -2, Noelin-4 has a hydrophobic leader sequence that is predicted to be cleaved after residue #26 in the sequence VLP-TN, removing the entire A region (arrowheads, Fig. 1B). This leaves essentially the M region as the mature protein since the Y exon encodes one glycine residue and then a stop codon. This analysis of the sequence suggests that Noelin-4 may be secreted and glycosylated.

Noelin-4 is a secreted protein

To determine whether Noelin-4 is a secreted protein, we expressed epitope-tagged constructs in *Xenopus* oocytes (Fig. 2A). Cellular and supernatant fractions were immunoprecipitated and compared (Fig. 2B). Full-length Noelin-4 with a carboxy-

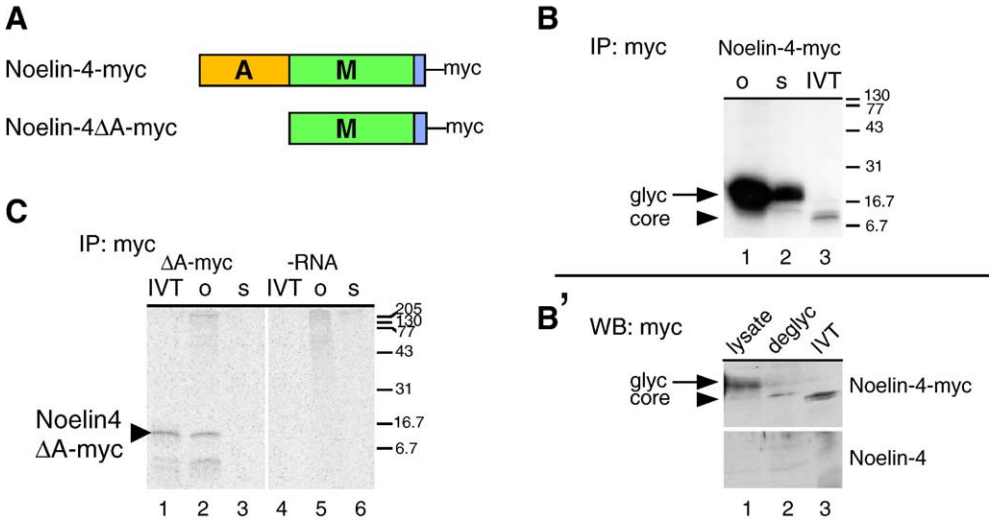

Fig. 2. Noelin-4 is a secreted, glycosylated protein. (A) Noelin constructs used in these studies are shown schematically. Noelin-4 was myc-tagged at the carboxy terminal. Noelin-4ΔA-myc is Noelin-4-myc with the A exon removed. (B) Noelin-4-myc was immunoprecipitated from oocyte (o, lane 1) and supernatant (s, lane 2) fractions. In vitro-translated protein (IVT) is shown in lane 3. Oocyte and supernatant fractions contain Noelin-4 protein that is larger than the size of in vitro-translated core protein. (B′) Anti-myc Western blot of embryos injected with *Noelin-4-myc* or *Noelin-4* (for a Western blot control) as indicated. Proteins were run on SDS-PAGE either as embryo lysate (lane 1), lysate treated with PNGase F (deglyc, lane 2) or in vitro-translated protein (IVT, lane 3). Proteins in the deglycosylated sample collapsed to the size of in vitro-translated protein. (C) Noelin-4ΔA-myc immunoprecipitated from the oocyte fraction only, and was not found in the supernatant fraction (lane 2 versus lane 3). Control oocytes and supernatant are shown in lanes 4–6.

terminal *myc* tag was observed in both the oocyte and supernatant fractions (Fig. 2B, lanes 1 and 2). The presence of Noelin-4 protein in the supernatant suggests that the hydrophobic leader sequence was indeed cleaved in vivo, allowing the protein to be secreted. The size of the oocyte-synthesized Noelin-4 protein was larger than that of the in vitro-translated protein (lane 3), suggesting that the former was glycosylated. In order to test this possibility, protein samples from *Noelin-4-myc* injected embryos were treated with a deglycosylating enzyme. When treated with PNGase F, the protein detected by anti-myc on a Western blot collapsed to roughly the size of in vitro-translated Noelin-4-myc (Fig. 2B′, lanes 2 and 3), while untreated sample ran more slowly through the gel (Fig. 2B′, lane 1). Together, these results show that Noelin-4 is a glycosylated protein.

Noelin-4 appears to be more robustly secreted than the previously characterized Noelin-1 isoform (Moreno and Bronner-Fraser, 2001). Noelin-1 and -2 contain the carboxy terminal sequence Ser–Asp–Glu–Leu (SDEL) which is likely responsible for their less efficient secretion (Moreno and Bronner-Fraser, 2001). This sequence is similar but not identical to the consensus sequence KDEL signal for protein retention in the endoplasmic reticulum of vertebrates, *Drosophila, C. elegans* and plant cells (Munro and Pelham, 1987).

To confirm that the A exon contains a signal sequence for Noelin-4 secretion, a construct lacking this portion of Noelin-4 (Fig. 2C, ΔA-myc) was generated (see Fig. 2A for schematic). Noelin-4ΔA-myc was synthesized in oocytes (Fig. 2C, lane 2) but was not secreted (lane 3). In addition, both the in vitro-translated and the in vivo-synthesized protein were the same size, indicating that they were not glycosylated (compare lanes 1 and 2). Thus, the A region with its hydrophobic leader sequence appears to be required for the secretion and thus glycosylation of Noelin-4.

Noelins are expressed early in development

To determine the temporal expression pattern of Noelin isoforms in *Xenopus*, we performed a developmental series of

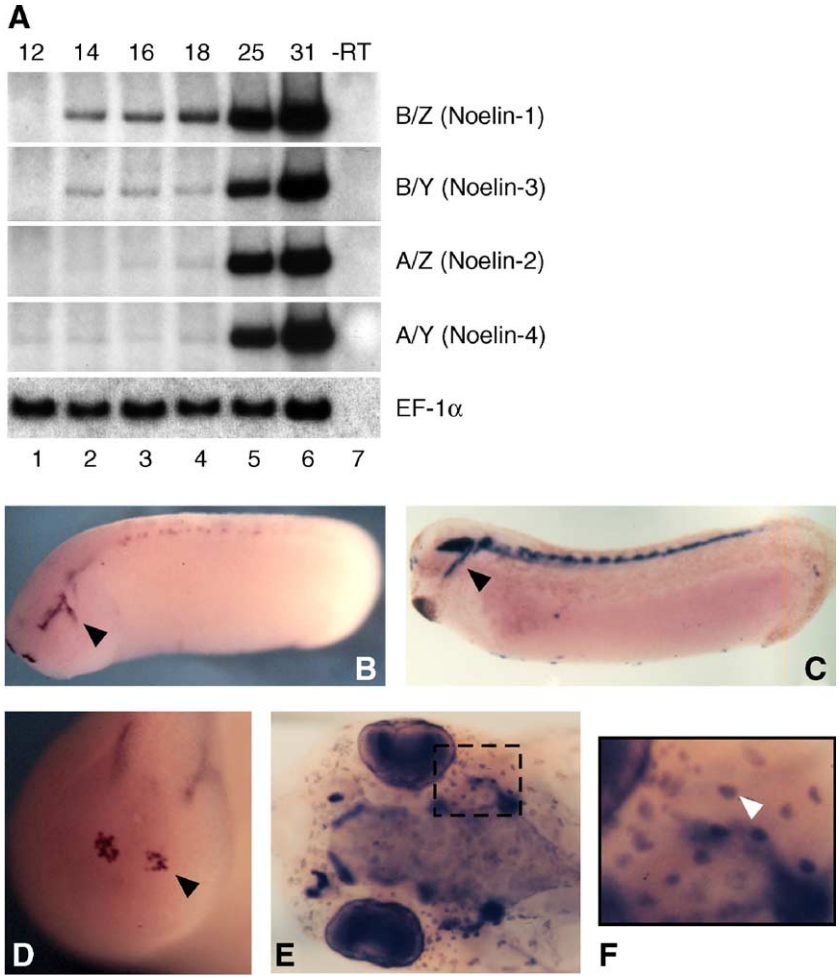

Fig. 3. Developmental expression patterns of *Noelins*. (A) *Noelin* temporal expression patterns. Embryos were harvested at the stages indicated and examined for the presence of the specific *Noelin* isoforms by RT-PCR. EF1α is a loading control, −RT is a control for genomic DNA contamination. Primer pairs used hybridize to only one splice variant each, as indicated. Noelin expression is observed weakly from neural plate stages, with strong expression from late neurula stages. (B–F) Spatial expression pattern of *Noelin-3/4* (Y exon in situ hybridization, purple staining). Anterior is to the left. (B) Side view of stage 27 embryo with staining in cranial ganglia (arrowhead) and spinal cord; (C) stage 29 embryo with staining in trigeminal ganglion (arrowhead) and spinal cord; (D) anterior view of stage 26 embryo highlighting olfactory placode expression (arrowhead); (E) dorsal view of stage 42 embryo with staining in cranial ganglia, eye, and neuromasts; (F) magnification of boxed region in panel D showing neuromast expression (arrowhead).

RT-PCR in stages ranging from late gastrulation (stage 12) through late tailbud (stage 31). Oligonucleotides directed to regions flanking the common central M exon revealed the temporal distribution of each of the isoforms (Fig. 3A). Interestingly, the B-containing isoforms, *Noelin-1* and *Noelin-3,* were observed from stage 14 onward, with increasing expression as development proceeds. The A-containing isoforms *Noelin-2* and *Noelin-4* were present at low levels through the same stages as the B-containing isoforms, and may be present at low levels even earlier. Like the B isoforms, the A isoforms were also strongly expressed by stage 25 (Fig. 3A, lane 5).

Noelin-3 and -4 are expressed in post-mitotic neural tissues

We previously showed that *Xenopus Noelin-1* and *-2* are expressed from stage 20 in post-mitotic neural tissues (Moreno and Bronner-Fraser, 2001). To examine the spatial expression pattern of *Noelin-3* and *-4*, whole mount in situ hybridization was performed with several probes from different regions of the sequences of *Noelin-3* (BMY) and *Noelin-4* (AMY). Results with the Y exon probe which marks *Noelin-3* and *-4* indistinguishably and which we refer to in this context as *Noelin-3/4*, are essentially equivalent to those obtained with the A, B and Z exons (Fig. 3B; Moreno and Bronner-Fraser, 2001, 2002). Expression was observed in post-mitotic neural tissues in the brain, spinal cord and cranial ganglia beginning at stage 21 (Figs. 3B–F and Moreno and Bronner-Fraser, 2001). At the latest stage examined, tadpole stage 42, expression was also observed in neuromasts and lateral line ganglia (Figs. 3E, F). Thus, the Y-containing *Noelin-3/4* isoforms mark post-mitotic neural cells in both the peripheral nervous system (cranial ganglia and lateral lines) and the central nervous system (eye, brain, spinal cord) as do the Z-containing *Noelin-1/2* isoforms.

Noelin-3/4 are induced by neurogenic genes

Neurogenesis is initiated by a neurogenic transcriptional cascade that activates and promotes neuronal differentiation. Ectopic expression of neurogenic genes causes neurons to develop in the epidermis. Since *Noelin* isoforms are expressed in post-mitotic neural tissues, we tested whether *Noelin-4* and its closely related splice variant *Noelin-3* were activated by the neurogenic cascade.

We observed that *Noelin-3/4* were up-regulated in ectopic neurons induced by both *XNeuroD* (see Fig. 4F) and *X-ngnr-1* (Fig. 4B, arrowhead). In general, all embryos injected with *X-ngnr-1* or *XNeuroD* displayed this phenotype (for one representative experiment: 96%, n = 25). Interestingly, *N-tubulin* appeared to consistently mark a greater number of neurons than did the *Noelin* isoforms suggesting that *Noelin* may mark a subset of neurons induced by neurogenic genes (compare Figs. 4A and B).

We next asked whether neurogenic genes could induce *Noelin-3/4* expression in the absence of mesoderm signals in animal cap explants. The common Y exon of *Noelin-3/4* was modestly induced in animal caps expressing *X-ngnr-1* (Fig. 4D) or *XNeuroD* (see Fig. 4F). *N-tubulin* was highly induced by *X-ngnr-1* (Fig. 4C). Control animal caps injected with *lacZ* did not express the Y exon (Fig. 4E). These results show that *Noelin-3/4* are induced by genes in the neurogenic cascade, both in whole embryos and in isolated animal caps, but much more robustly in the former.

In order to precisely determine which isoforms were induced by *X-ngnr-1* and *XNeuroD*, we performed RT-PCR on induced animal caps using primers that specifically target each isoform (as in Fig. 3). All four isoforms were induced in animal caps by stage 22 (Fig. 4F), confirming our previous results that both *Noelin* A forms and both *Noelin* B forms are induced by neurogenic genes.

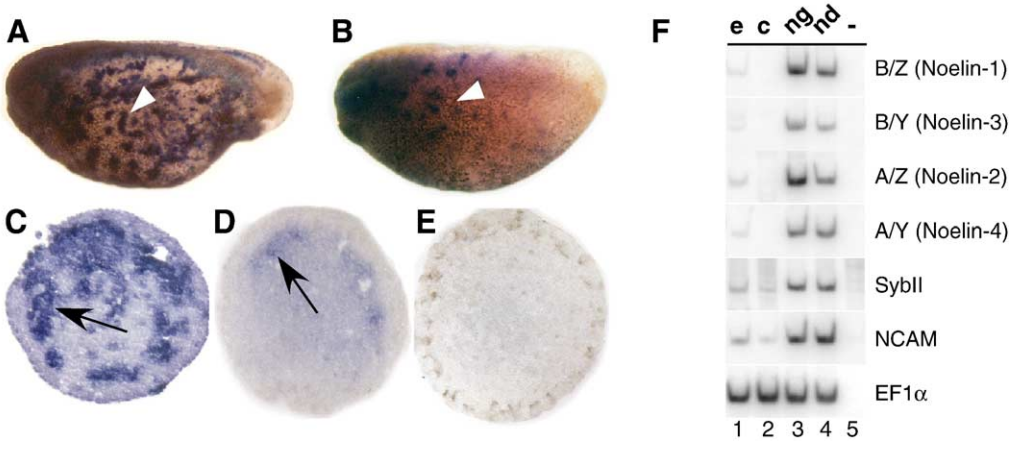

Fig. 4. *Noelin-3* and *-4* are induced by neurogenin. (A, B) Embryos were injected in one cell at the two-cell stage with 100 pg of *X-ngnr-1* and cultured to stage 24. Whole mount in situ hybridization for *N-tubulin* (A) or the Y exon of *Noelin-3* and *-4* (B) is shown. Ectopic neurons staining with the markers are indicated with arrowheads. (C–E) cross-sections of animal caps from embryos injected with 100 pg *X-ngnr-1* or *lacZ* in 2/2 cells, excised at stage 9 and cultured to stage 22. Arrows point to regions staining with the markers. (C) *N-tubulin* staining; (D) Y exon staining; (E) *lacZ*-injected, *N-tubulin* staining. Embryos for this experiment were derived from pigmented mothers; brown color is due to pigment granules. (F) RT-PCR on stage 22 animal caps explanted at stage 10, derived from embryos injected with *lacZ* (c, lane 2), *X-ngnr-1* (ng, lane 3), or *XNeuroD* (nd, lane 4), or on whole embryo controls (e, lane 1). Both *XNeuroD* and *X-ngnr-1* induced expression of all four Noelin isoforms. RNA without reverse transcriptase was used as a negative control (–, lane 5). Primers used are indicated; each *Noelin* set hybridizes to only the indicated isoform. SybII = *synaptobrevinII*, a marker for differentiating neurons (Knecht et al., 1995).

Noelin-4 over-expression in embryos causes neural expansion

To examine the possible function of *Noelin-4* in the embryo, we first performed gain-of-function experiments. 85% of embryos injected with doses of *Noelin-4* mRNA ranging from 500 pg to 1 ng exhibited abnormal development of the nervous system. The majority of embryos displayed enlarged neural tissues and/or ectopic cement glands and pigment cells. The observed phenotypes are summarized in Table 1. When embryos were injected with 500 pg of *Noelin-4* mRNA in one blastomere at the 2-cell stage, there was a unilateral expansion of neural tissue (Table 1), manifested as asymmetrical neural plate. Staining with the pan-neural marker *Sox-2* at stage 16 revealed considerable enlargement of the neural plate on the injected side (Fig. 5A). In contrast, sibling control embryos injected with *Noelin-2* (AMZ) or *lac*Z had normal-appearing, symmetric neural plates (Figs. 5B and C). At later stages, retinas and spinal cords were enlarged on the injected side (Figs. 5D–G and data not shown).

The *Noelin-4*-induced expansion of neural territories, especially in the retina, caused further secondary defects in older embryos. Normally, the optic vesicles evaginate to form the optic cup beginning at stage 29. *Noelin-4* over-expression often caused enlargement of the retina in both circumference and thickness and a delay in evagination (Figs. 5F, G). In addition to neural/retinal expansion, a high percentage of injected embryos exhibited a mild axial dorsalization (i.e., reduction of tail structures, bent axis) and spina bifida (open spinal cord; see Table 1). There appeared to be loss of ventral/posterior fates with a concomitant increase in dorsal/anterior fates.

The phenotype after *Noelin-4* over-expression was dose-dependent. At higher doses, an increased frequency and severity of phenotype was observed, with as many as 50% of embryos exhibiting enlarged neural structures, failure of neural tube closure and ectopic development of *Sox-2*-expressing structures ($n = 185$ in five separate experiments; see also Table 1; Fig. 5O).

Table 1
Noelin-4 over-expression phenotypes

Phenotype	% experimental/ % control
Enlarged retina	38/0
Enlarged neural tube	33/0
Ectopic cement gland	18/0
Ectopic pigment cells	10/0
Retinal pigmented epithelium extending into midbrain	15/2
Ectopic neural structures	10/0
Spina bifida	41/2
Bifurcated tail	18/0
Disorganized/missing anterior neural structures	18/0
Normal	15/94

Over-expression phenotypes observed for *Noelin-4*. Two experiments were combined (injected embryos $n = 100$, control embryos $n = 50$) and data were tabulated for both. Most embryos displayed multiple phenotypes. Cement glands, pigment cells, and retinal pigmented epithelium extension were scored by visual inspection of unstained whole mounts. Enlarged neural tube and retina, as well as ectopic neural structures, were scored by *Sox-2* staining appearance. Control embryos were injected with similar doses of *lac*Z mRNA.

Frequently, embryos had ectopic cement glands (see Table 1; Figs. 5M, O) that were discontinuous with the endogenous ones and always located on the head ectoderm, typically near the eye or over the branchial arches. The retinal pigmented epithelium (RPE) sometimes was expanded into the midbrain in embryos with anterior injections (data not shown) and ectopic, pigmented *Sox-2*-positive regions with the appearance of ectopic RPE were observed (Figs. 5N, O, and see Table 1). By contrast, embryos injected with the same doses of *Noelin-1, Noelin-2* or *lac*Z mRNA appeared normal, indicating that these results were specifically due to the over-expression of *Noelin-4* (see Table 2).

The *Noelin-4* over-expression phenotype appears to be sensitive to the level of *Noelin-4* seen by the tissues affected. The activity of the lineage tracer β-galactosidase indicates an area of concentration of the injected mRNA; the actual spread of the injection may be over a much greater area. In our experiments, lineage tracer-positive cells generally were found surrounding but not necessarily within ectopic neural, *Sox-2*-positive tissue; however, ectopic cement glands always contained high levels of the lineage marker.

Since we observed an increase in neural precursors, we also examined whether *Noelin-4* over-expression caused an increased number of neurons to differentiate. Embryos stained with the pan-neuronal marker *N-tubulin* did not exhibit any increase in the number of neurons or any ectopic neuronal differentiation (Figs. 5P–S). Thus, *Noelin-4* over-expression causes an increase in the neural precursor population but does not promote greater numbers of neurons to differentiate. Interestingly, we observed that in a modest number of injected embryos ($n = 12/50$), *N-tubulin* expression in the neural plate was reduced in the lateral stripe containing sensory neuron precursors (compare Figs. 5P and Q). By later neurula stages, *N-tubulin* expression recovered and no decrease was noted (Fig. 5R).

Since changes in the underlying mesoderm could explain the expansion of the neural tissues, we examined the effects of over-expressed *Noelin-4* on mesoderm. First, we performed RT-PCR on animal caps from embryos injected with *Noelin-4* at doses that caused severe neural patterning defects. The mesoderm marker *muscle actin* (*MA*) was not induced (Fig. 6A, lane 4). This suggests that *Noelin-4* cannot induce mesoderm to form in this context. We also determined that *Noelin-4* is not a direct neural inducer (such as *noggin* or *chordin*; Harland, 2000), since it did not induce neural marker expression in animal caps (*NCAM*, Fig. 6A, lane 4).

Next, we examined the effects of *Noelin-4* injection on mesoderm in whole embryos. Cross-sections through all axial levels revealed no specific deformities in the developing mesoderm (see Fig. 5). In situ hybridization for *MA*, which marks paraxial mesoderm, failed to show obvious changes in *MA* in the mesoderm (Figs. 6B, C). Thus, the neural patterning defects caused by *Noelin-4* cannot be attributed to changes in the underlying mesoderm.

Noelin-4-induced neural expansion is not mediated by increased proliferation or loss of cell death

Two possible explanations for the neural expansion observed after over-expression of *Noelin-4* are that there was an

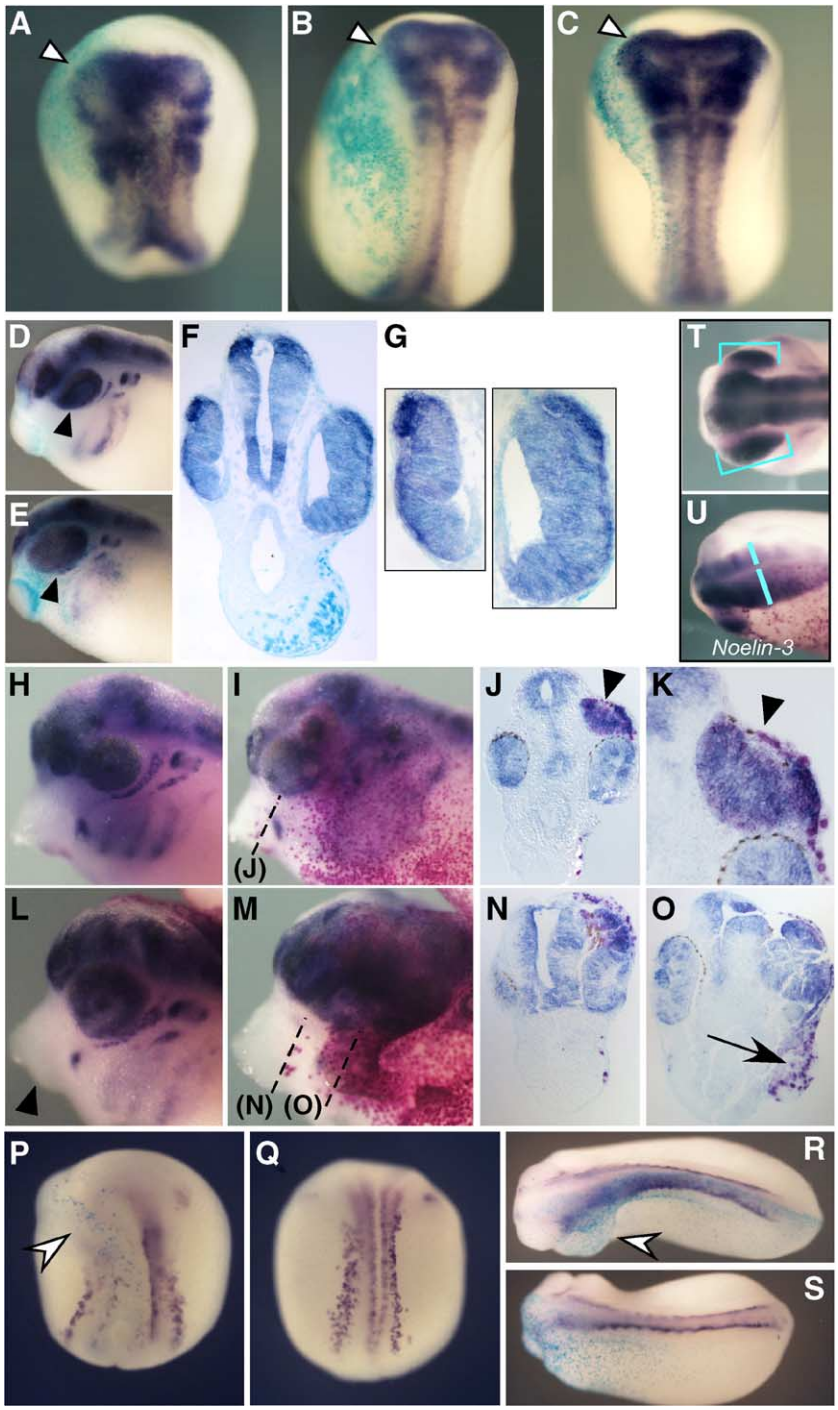

Fig. 5. *Noelin-4* over-expression results in expansion of neural fate. Embryos injected with Noelin-4 exhibit enlarged and ectopic neural tissue. Embryos were injected with 500 pg (A–G, P–S) or 1 ng (H–O) of *Noelin-4* mRNA, 500 pg *Noelin-3* (T, U), and 100 pg of *lac*Z mRNA as a lineage tracer. β-galactosidase activity was assessed with X-gal (turquoise, A–G) or Magenta-Gal (magenta, H–O) and embryos were stained for *Sox-2* expression. (A–C) Neural plate stage embryos injected with (A) *Noelin-4 (*AMY*)*, (B) *Noelin-2* (AMZ) or (C) *lacZ.* Injected side is to the left, embryos are photographed from the dorsal side, oriented with anterior pointing up. Anterior neural plate is indicated with an arrowhead. Note expansion of the neural plate in panel A. (D–G) Embryos were harvested at stage 29 and stained for *Sox-2* expression. (D) Control side, (E) injected side of same embryo. Neural retina is revealed by *Sox-2* staining, note that injected side eye is larger than control side (arrowheads). (F) Cross section through midbrain region; (G) comparison of neural retinas from both sides of the embryo magnified to the same degree. (H–O) Examples of embryos harvested at stage 35 and stained for *Sox-2* expression. (H, L) Control side; (I, M) injected side. Panels J, N, and O are cross-sections through the head regions with the section level indicated on panels I and M. Panel K is a magnification of the injected side in panel J. Note expansion of neural tissue and ectopic *Sox-2* staining (arrowhead). Panel O shows an ectopic cement gland ventral to the eye (arrow) that is discontinuous with the endogenous cement gland (see arrowhead in panel M). (P–S) *N-tubulin* staining of embryos injected with *Noelin-4* (P, R) or *Noelin-1* (Q, S). (P, Q) Neural plate stage embryos, with injected side to the left, anterior pointing to top. (R, S) Embryos at stage 24 with anterior to the left. Arrowheads indicate bulging tissue on the injected side in panels P, R. (T, U) Noelin-3 causes similar neural territory expansion. *Noelin-3* (BMY) injection, *Sox-2* staining. Bars and brackets outline width of neural structures in two different embryos on the injected side (bottom half) and uninjected control side (top half).

Table 2
Noelin-1 rescues *Noelin-4* phenotype

Phenotype	N4 (high)	N4 + N1 (high:high)	N1 (high)	N4 (low)	N4 + N1 (low:high)
Ectopic cement gland	32%	6%	0	5%	0%
Enlarged neural tissue	50%	15%	0	51%	18%
Severity	***	**	n/a	**	*
Spina bifida	26%	3%	0	3%	3%
Number of embryos	50	34	67	37	40

Co-expression phenotypes of *Noelin-1* and *Noelin-4*. *Noelin-1* and/or *Noelin-4* mRNAs were injected as indicated, with relative doses of 1:3 or 1:1 (RNA: water or co-expressed RNA) by RNA concentration. Embryos were scored visually at stage 31. N1 = *Noelin-1*, N4 = *Noelin-4*. Injection of equivalent doses of N4 and N1 (high:high) resulted in a reduced incidence of the N4 phenotype. Reducing the dose of N4 reduced the frequency of the phenotype (compare N4 [high] to N4 [low]). A low dose of N4 plus a high dose of N1 also reduced the frequency of the low-dose N4 phenotype. Severity of phenotype was scored with *** being most severe.

increase in cell proliferation and/or a decrease in cell death. To address the first possibility, we tested whether there was increased proliferation in *Noelin-4*-expressing cells using the mitosis marker anti-phospho-histone H3, which labels cells in and shortly after metaphase (Saka and Smith, 2001).

Embryos were injected with *Noelin-4* mRNA (500 pg) to induce the neural expansion phenotype and examined for alterations in cell division. At stage 14 and again at stage 24, no evidence of increased mitosis was observed by phospho-histone H3 staining (stage 14: $n = 4$, stage 23: $n = 4$ Figs. 6D, E) either in whole mount or in sections by analyzing the number of cells in metaphase (Figs. 6F, G). To determine whether a loss of cell death might play a role in the expansion of neural fate in Noelin-4-injected embryos, we examined them with TUNEL staining. *Noelin-4*-injected embryos were indistinguishable by TUNEL staining from control embryos, suggesting that there was no decrease in cell death (Figs. 6H, I; $n = 8$ embryos per condition).

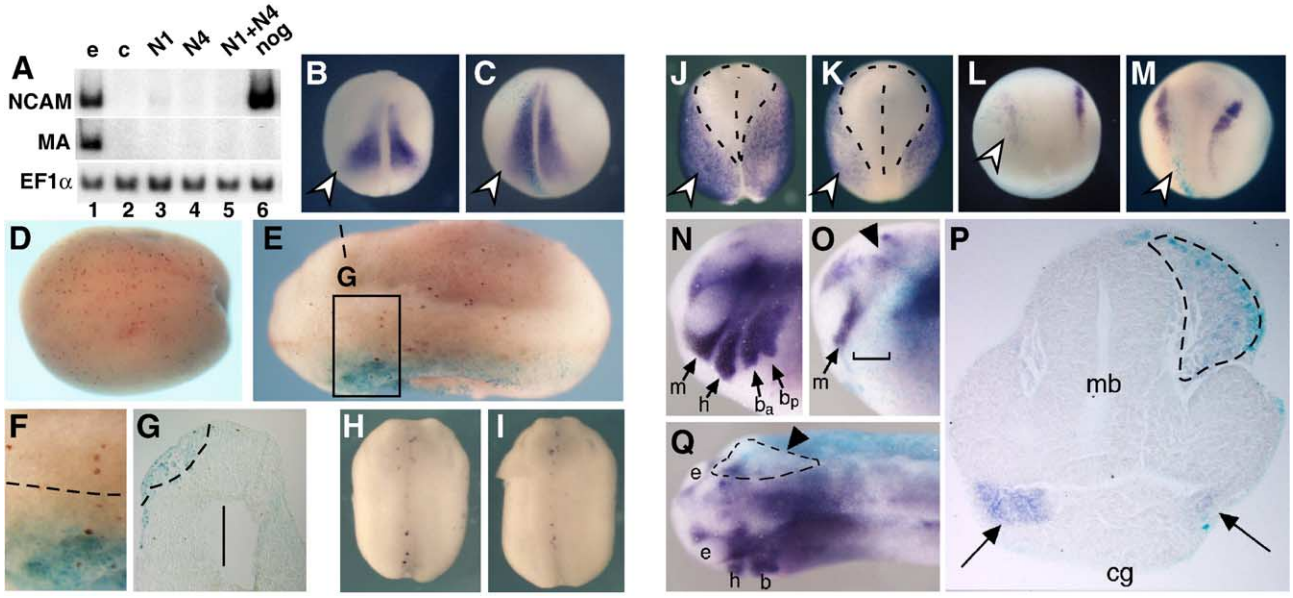

Fig. 6. Ectoderm in *Noelin-4* embryos is diverted toward a neural fate. (A–C) Mesoderm is not induced by *Noelin-4*. (A) RT-PCR of animal caps injected with the indicated isoform (N1 = *Noelin-1*, 500 pg; N4 = *Noelin-4*, 500 pg; N1 + N4 = 500 pg each; nog = 100 pg *noggin*; e = stage 22 embryo control; c = 500 pg *lac*Z-injected animal cap control). *NCAM* indicates neural induction, *MA* (*muscle actin*) indicates mesoderm. *EF1α* is a loading control. (B, C) Mesodermal MA expression is not affected by Noelin-1 over-expression. Neural plate stage embryos injected and stained for *MA*: (B) stage 15 embryo injected with *Noelin-4* (1 ng); (C) Noelin-1 injected stage 16 (1 ng). Arrowheads indicate injected side. (D–G) Anti-phospho Histone H3 staining of embryos injected with *Noelin-4* (500 pg) and *lac*Z (50 pg). No difference in proliferation was observed. (D) Neural plate stage embryo, anterior to the left, injected side down. Brown dots indicate anti-phospho Histone H3 positive cells. (E–G) Stage 24 embryo. (E) Anterior to the left, injected side down. (F) Closeup of dorsal view (boxed area in panel E, midline marked by dashed line); (G) cross section (level of section indicated in panel E) with midline of embryo marked by vertical line. Note the expansion of tissue on injected side in panel F (below dotted line), which contains no extra proliferative figures. (H, I) Cell death assay of *Noelin*-injected embryos. TUNEL staining of embryos injected in 2 of 2 cells with 500 pg *Noelin-4* (H, stage 17) or *lac*Z (I, stage 18). Anterior is oriented up. No change is noted in TUNEL staining between these embryos ($n = 8$ each). (J, K) Conversion of epidermal territory. Embryos injected with 1 ng *Noelin-4* (J, stage 16) or *Noelin-1* (K, stage 15) and stained for *epidermal keratin*. Neural plate territory and midline are indicated with dashed line; injected side is to the left (arrowheads). In panel J, note that the neural plate remains larger on the injected side. (L–Q) Neural crest formation is perturbed by *Noelin-4* over-expression. Embryos were injected with 1 ng *Noelin-4* and stained for the neural crest marker *XSlug* (L, M) or *XTwist* (N–Q). (L) Stage 15 embryo, *Noelin-4*-injected side is to the left (arrowhead). Note the loss of *XSlug* staining on the injected side. (M) Stage 16 embryo injected with *Noelin-1* (*BMZ*). (N) Control side; (O) injected side; note missing streams of neural crest staining (bracket) and overgrown tissue near neural tube (arrowhead). (Q) Dorsal view, with overgrown tissue outlined (arrowhead). (P) Cross section of a similar embryo shows mandibular neural crest staining is missing from injected side (arrows). Extra tissue formed by *Noelin-4* ectopic expression (dashed outline) is negative for *XTwist* expression. m, mandibular crest; h, hyoid crest, b_a and b_p: anterior and posterior branchial crest; e, eye; cg, cement gland; mb, midbrain.

Noelin-4 causes expansion of neural tissue at the expense of presumptive epidermis and neural crest

Another possible explanation for the observed expansion of the nervous system is that it results from conversion of other ectodermal cell fates (epidermal ectoderm and/or neural crest) into neuroepithelium. In support of this possibility, numerous islands of ectopic *Sox-2*-positive cells were observed within the epidermal ectoderm (Figs. 5H–O). Occasionally, these *Sox-2*-expressing regions in the epidermis formed structures with the appearance of otic vesicles as well as lateral extensions of the neural tube. When examined in cross-section, these neural tissues appeared in the epidermal ectoderm and were not associated with any morphological indication of ectopic or mispatterned mesoderm (Fig. 5J and data not shown). Furthermore, staining of injected embryos with the epidermal marker *epidermal keratin* (*EK*) revealed that the expanded neural plate occupied territories that normally contain presumptive epidermis, suggesting that the neural ectoderm in *Noelin-4*-injected embryos expanded at the expense of the epidermal ectoderm (Figs. 6J, K).

To examine how the ectoderm-derived neural crest was affected after *Noelin-4* over-expression, embryos were analyzed with the neural crest markers *XSlug* (Mayor et al., 1995) and *XTwist* (Hopwood et al., 1989). *Noelin-4*-injected embryos exhibited reduced staining of both markers on the injected side, and were sometimes missing individual neural crest streams as assayed by *XTwist* staining (Figs. 6L–P, *XTwist*: n = 14/17; *XSlug*: n = 16/22). For example, the hyoid and branchial neural crest streams typically were absent (Fig. 6N), while the mandibular crest stream around the eye was present but reduced in size (Figs. 6O, P). In contrast, neural crest formation and migration appeared normal in control embryos (*XTwist*: n = 17/17, *XSlug* 21/22) and on the uninjected side of *Noelin-4*-injected embryos (Figs. 6L–O). These results suggest that, in addition to epidermal conversion, over-expression of *Noelin-4* may divert presumptive neural crest to neural fate.

Noelin-4 binds Noelin-1

Our previous studies on Noelin-1 suggested that it might have binding partners either within the cell or in the extracellular environment (Moreno and Bronner-Fraser, 2001). Under non-reducing gel conditions, Noelin-1 protein (predicted size 56 kDa) ran as a band larger than 205 kDa. We hypothesized that because of the similarities between Noelin-1 and olfactomedin, a protein that forms multimers in the extracellular matrix, Noelin-1 may also form multimers with itself or other protein partners. Olfactomedin multimerizes through a pair of cysteine residues (Yokoe

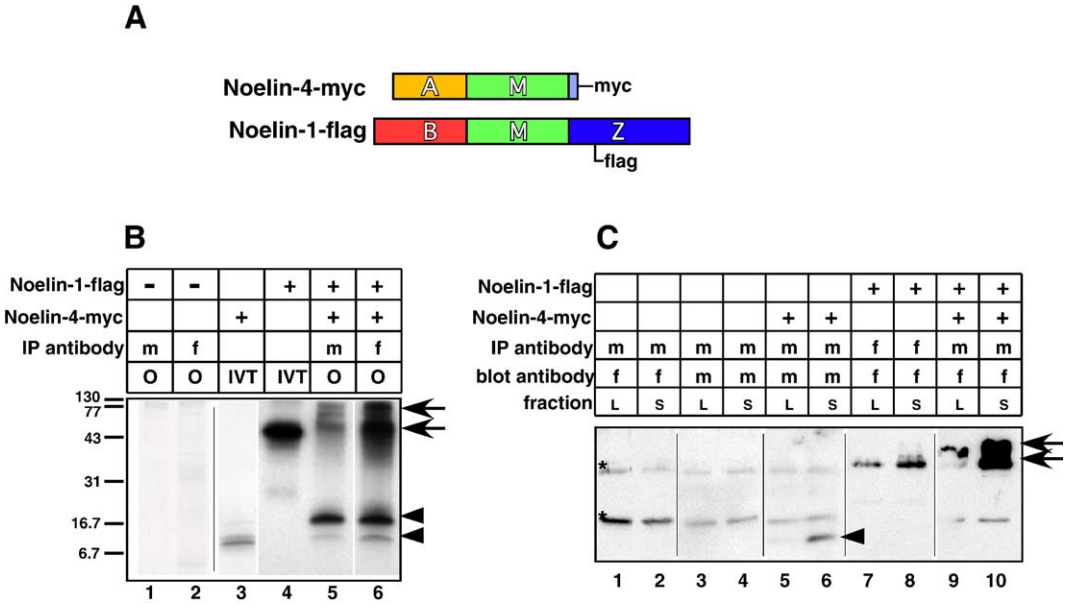

Fig. 7. Noelin-4 binds to Noelin-1. (A) Noelin-4-myc and Noelin-1-flag constructs used are shown diagrammatically. Noelin-1 bears an internal Flag epitope when designated with a plus sign (+), or is without a tag when designated with a minus sign (−). O, oocyte; IVT, in vitro-translated protein; m, myc; f, flag. (B) Co-immunoprecipitation assay in *Xenopus* oocytes. Oocytes were injected as indicated and cultured in the presence of ^{35}S-methionine. Oocyte controls were injected with an untagged version of Noelin-1 and immunoprecipitated with either myc or flag (lanes 1, 2). In vitro-translated proteins (lanes 3, 4) are compared to oocyte-translated proteins (lanes 5, 6). Samples were immunoprecipitated with the indicated antibody (m = myc; f = flag). Noelin-4-myc is indicated with arrowheads; Noelin-1-flag is indicated with arrows. (C) IP-Western blot. COS-7 cells were transfected with the indicated plasmids and then immunoprecipitated with either myc or flag antibodies. Lysate (L) and supernatant (S) fractions were then resolved on SDS-PAGE and transferred to nitrocellulose before enhanced chemiluminescence detection with the indicated antibody. Some of the precipitating antibodies were also eluted during sample preparation; heavy and light-chain immunoglobulin bands detected with the Western secondary antibody are indicated with asterisks in control lane 1. Noelin-4-myc is denoted with an arrowhead; Noelin-1-flag is denoted with arrows. Myc pull-down of Noelin-4-myc samples brought down a band that immunoreacted with myc on the Western blot (arrowhead, lanes 5, 6), as did flag pull-down on samples transfected with Noelin-1-flag and subsequently blotted for flag (lanes 7, 8). Samples transfected with both plasmids and immunoprecipitated with anti-myc contained flag-immunoreactive bands at the size of Noelin-1-flag (arrows, lanes 9, 10).

and Anholt, 1993) which are conserved in the four Noelin isoforms.

To determine whether Noelin isoforms could interact, we co-expressed differentially tagged *Noelin-4* and *Noelin-1* constructs and then immunoprecipitated with antibodies to the different epitope tags. The *Xenopus Noelin-4* construct contains a carboxy terminal myc tag; this was co-expressed with a Noelin-1 construct bearing an internal flag epitope (Fig. 7A).

Co-injected oocytes made proteins of the expected sizes for both Noelin-4 and Noelin-1 (Fig. 7B, in vitro-translated proteins lanes 3, 4). The results in Fig. 7 show that immunoprecipitation of Noelin-4-myc co-precipitates a band of the size of Noelin-1-flag, and vice versa. In oocyte fractions, the greatest portion of immunoprecipitated Noelin-4 migrated at approximately 22 kDa, with a weaker band found at about 11 kDa (Fig. 7B, lanes 5 and 6 Noelin-4 bands). Immunoprecipitated Noelin-1 ran at approximately 60 and 77 kDa for the cellular and secreted forms, respectively (lanes 5 and 6; (Moreno and Bronner-Fraser, 2001). The identity of these bands was confirmed by immunoblot analysis against the reciprocal proteins in tissue culture cells. Briefly, COS-7 cells transfected with both *Noelin-4-myc* and *Noelin-1-flag* were immunoprecipitated with either myc or flag antibody, followed by Western blotting with the reciprocal antibody (Fig. 7C). Pull-down with anti-myc antibody co-precipitated an anti-flag reactive protein of the expected size for Noelin-1-flag (Fig. 7C, lanes 9 and 10). Thus, we find that in Noelin-4 and Noelin-1 can form complexes in *Xenopus* oocyte and cell culture assay systems.

Noelin-4 and Noelin-1 functionally interact

The biochemical results showing that Noelin-1 and Noelin-4 can bind in cell-based assays suggested that they might functionally interact in vivo. To test this, we co-injected *Noelin-4* and *Noelin-1* mRNAs in varying ratios and then examined the subsequent embryonic phenotypes. Interestingly, the data show that *Noelin-1* rescues the abnormalities caused by *Noelin-4* over-expression (Table 2), resulting in a marked decrease in the percentage of embryos exhibiting defects. *Noelin-1* co-injection reduced the frequency of these phenotypes approximately 3- to 8-fold. In contrast, *Noelin-1* alone caused no obvious morphological or gene expression phenotype (see Figs. 5B, Q, S, and 6C, K, M and Table 2). These results indicate that in vivo, *Noelins* may interact and *Noelin-1* may negatively regulate *Noelin-4*.

Noelin short isoforms have similar functions

With the exception of 30 additional amino acids in the amino terminus, *Noelin-3* and *-4* share all structural features, including the conserved cysteine residues in the M region, M region glycosylation site and hyaluronate binding sites (see Fig. 1A). Furthermore, Noelin-3 contains the same signal peptide sequence (B region) that is cleaved to yield a secreted protein in the case of Noelin-1 (Moreno and Bronner-Fraser, 2001). To test whether they had similar functions, we compared the effects of *Noelin-3* over-expression in whole embryos to that of *Noelin-4*. The over-expression phenotype of *Noelin-3* was similar to that of *Noelin-4* in these assays. 500 pg of *Noelin-3* mRNA microinjected into one blastomere at the 2-cell stage gave rise to embryos exhibiting expansion of neural tissue similar to that seen with *Noelin-4*. In the anterior neural tube, expanded domains containing *Sox-2*-positive cells were observed in neural tubes on the injected side (Fig. 5U). Over-expression in the region of the eye caused enlarged retina formation (Fig. 5T). These results suggest that *Noelin-3* and *Noelin-4* function in like fashion.

To further test whether *Noelin-3* might be functionally similar to *Noelin-4* in terms of the ability to be rescued by *Noelin-1*, we again performed co-injection experiments. Embryos exhibited a clear reduction in the neural expansion phenotype when *Noelin-1* was co-injected with *Noelin-3*, as was the case for *Noelin-4* and *Noelin-1* co-expression (Table 3). Thus, the Y-form splice variants *Noelin-3* and *-4* have similar activities. Taken together, these data suggest that interacting Noelin isoforms may modulate one another's functions in vivo and promote certain fate choices depending on the balance of these factors in the cell.

Discussion

Our characterization of *Noelin-4* function in the early *Xenopus* embryo suggests that it acts as a factor that promotes neural precursor fate. Since over-expression of *Noelin-4* caused expansion of neural tissues but did not induce ectopic neurogenesis, an endogenous function of this glycoprotein may be to maintain neuronal precursors in a pre-differentiated state until the appropriate time to continue differentiation. The biochemical interaction of Noelin-4 with Noelin-1 coupled with the ability of Noelin-1, a neurogenesis promoting factor, to modulate this maintenance activity suggest an interesting reciprocal mechanism by which the balance of these family members in a differentiating cell determines the precursor versus differentiated state. Our results are also consistent with the possibility that Noelin-4 may titrate the neurogenesis-promoting effects of Noelin-1 until the appropriate time for differentiation to proceed. This

Table 3
Noelin-3 acts similarly to *Noelin-4* and is rescued by *Noelin-1*

Phenotype	N3	N3 + N1	N4	N4 + N1	N1	*lac*Z
Enlarged/Ectopic neural tissue	72%	32%	68%	21%	6%	0%
Severity	**	*	**	*	*	n/a
Number of embryos	36	47	44	39	35	38

Co-injection with *Noelin-1* reduces the phenotype frequency for both *Noelin-3* and *Noelin-4*. 1 ng *Noelin-3* was injected with or without *Noelin-1*, in one cell at the two cell stage. *Noelin-4* was injected in one of two cells as in the low dose experiment shown in Table 2, with or without *Noelin-1*. The phenotypes counted in the scores include enlarged neural tissue, ectopic Sox-2 staining, and ectopic cement gland, which were visualized at stage 31–33. N1 = *Noelin-1*, N3 = *Noelin-3*, N4 = *Noelin-4*. The data represented here are from one injection experiment; embryos exhibited combinations of the scored phenotypes.

highlights the intriguing idea that interactions among members of this family of secreted proteins may play a regulatory role in modulating the timing of neuronal differentiation in the early embryo.

Noelin-4 over-expression induces neural expansion

Excess *Noelin-4* expression resulted in expansion of the neural plate, later causing an array of phenotypes including enlarged retinas and neural tubes, ectopic cement glands and otic-like vesicles (see Table 1 and Fig. 5). Most of the tissue expansion occurred in neural precursor cells as detected by *Sox-2* staining (Mizuseki et al., 1998b). This neural expansion did not occur via increased proliferation or loss of cell death. Instead, ectodermal tissues such as the cranial neural crest and epidermis appeared to be reduced and replaced by ectopic *Sox-2*-positive neural tissue in areas of *Noelin-4* over-expression. These results suggest that phenotypes observed with over-expression of *Noelin-4* are a conversion of non-neural or neural crest fates toward a neural fate. Further support for this idea comes from the presence of ectopic *Sox-2*-positive neural structures in the epidermis at high doses of *Noelin-4* (see Figs. 5 and 6N–P).

Noelin isoforms are induced by the neurogenic cascade

The timing of neuronal differentiation is an integral aspect of nervous system development. In order for the proper circuitry to form, neurons must be born and differentiate in a specific manner and order. The bHLH transcription factors *neurogenin* and *NeuroD* have neurogenic activity and play important roles in neurogenesis in the early *Xenopus* embryo (Brunet and Ghysen, 1999; Chang and Hemmati-Brivanlou, 1998). When *NeuroD* or *neurogenin* are expressed in the epidermis, they cause ectopic differentiation of neurons therein (Lee et al., 1995a; Ma et al., 1996). We previously showed that ectopic expression of either *X-ngnr-1* or *XNeuroD* induced expression of *Noelin-1/2* isoforms (Moreno and Bronner-Fraser, 2001). In this study we show that *Noelin-3/4* isoforms are also induced by over-expression of these neurogenic genes (Fig. 3). Because they are expressed in post-mitotic neurogenic tissues, the finding that Noelin proteins can interact and modify one another's functions suggests a novel way for neuronal differentiation to be regulated. *Noelin-1* promotes earlier neuronal differentiation in neuralized animal caps (Moreno and Bronner-Fraser, 2001). This, coupled with our results showing that *Noelin-4* over-expression promotes neural plate expansion (*Sox-2*) and a delay in neuronal marker expression (*N-tubulin*), suggests that endogenously, Noelin proteins could interact functionally and thereby regulate the timing of differentiation in neuronal precursors.

Noelin functional domains

Our results here and in previous work suggest that two separate functional domains reside in the Noelin proteins: a neural expansion/maintenance activity that is found in the M region, and a differentiation activity that resides in the Z region (Moreno and Bronner-Fraser, 2001). All Noelin isoforms contain the M region but differ in their upstream and downstream exons. The longer, Z-region-containing isoforms *Noelin-1* and *-2* can promote neurogenesis, but do not themselves act as neural maintenance factors. The shorter, Y-containing isoforms, *Noelin-3* and *-4* act to maintain and expand the neural precursor territory but do not promote neuronal differentiation. Since the Y exon codes for one glycine residue and then a stop, while at the amino terminal, all of the A region and much of the B region are cleaved during secretion, the Noelin-3/4 isoforms essentially are composed of the M region. The Z region, which is large (329 amino acids) and has five glycosylation sites (Barembaum et al., 2000; Moreno and Bronner-Fraser, 2001), may act to block or sterically hinder the M region on the same molecule. This could also explain why the Z isoforms do not act as neural maintenance factors even though they contain the common M region.

Noelin isoforms are expressed from neural plate stages onward as assayed by RT-PCR (see Fig. 3). Later in development, all isoforms are seen in post-mitotic neurogenic tissues in the brain, spinal cord and cranial ganglia. The expression profile of these isoforms is complicated by the fact that the two Z-containing isoforms (*Noelin-1* and *-2*) are made by two different promoters, as are the two Y-containing isoforms (*Noelin-3* and *-4*); in other words, a Y- and a Z-containing isoform are both transcribed from the same promoter, so that whenever a cell transcribes *Noelin-1* (BMZ), it also transcribes *Noelin-3* (BMY). We observed no differential regulation of the isoforms. Because of these transcriptional and splicing properties of the Noelins, it is difficult to examine the individual functions of Y-containing (short) or Z-containing (long) isoforms in vivo with morpholino antisense oligonucleotides since a long and a short form share the same 5′ exon.

Further levels of post-translation regulation, or of splicing mechanisms and mRNA stability may play an important role in modulating the expression levels of each isoform. Evidence for this hypothesis comes from the chick system, where the Y-containing isoforms are expressed later than the Z-containing isoforms, even though both A and B promoters transcribe Y and Z isoforms (Barembaum et al., 2000). This implies a level of splicing or mRNA stability regulation that we have not observed in *Xenopus*; however, it also suggests the existence of an as-yet-unknown mechanism for specific regulation of splice forms.

Noelin proteins interact and modulate partner function

The endogenous co-expression of *Noelin* isoforms suggests that they could function together in vivo. Our data demonstrate that *Noelin* isoforms biochemically bind to one another, since even the shortest isoform, Noelin-4, can bind Noelin-1 in immunoprecipitation assays. This suggests that the conserved cysteine residues in the M region are responsible for dimerization between Noelin isoforms as they are in olfacto-

medin (see asterisks, Fig. 1A). This physical interaction and implications from the data regarding the different functional domains of Noelin isoforms suggest that they may act as cofactors in vivo.

We further showed that the activity of *Noelin-4* in gain-of-function experiments was modulated by co-expression of *Noelin-1*. There are several possible mechanisms whereby interaction between the isoforms could modulate their activities. The large, Z-containing isoforms, which are known to be rather poorly secreted (Moreno and Bronner-Fraser, 2001), could act to restrict secretion of the Y-containing isoforms by binding them in the endoplasmic reticulum and thus preventing their efficient secretion. This could regulate the neural maintenance effects of these isoforms. Alternatively, the Z-containing isoforms, which are highly glycosylated, could act as anchors in the extracellular matrix for the smaller Y-containing isoforms, to maintain them in a specific area instead of allowing them to disperse. This could provide a local concentration for the Y isoforms to exert their effects. Moreover, these two proposed mechanisms could operate in concert, with the Z isoforms slowing the secretion of the Y isoforms, and then maintaining them in a local area for further activity. Our over-expression experiments may have disrupted the balance of the in vivo ratio of Y and Z, allowing this gain-of-function phenotype to be revealed.

Other olfactomedin family proteins modulate each other's functions

An important structural feature of the Noelin proteins is the olfactomedin domain. This region, contained in the C-terminal of the Noelin-1 and -2 isoforms, is related to similar domains in several proteins: MYOC/TIGR, a secreted protein in the aqueous humor of the vertebrate eye (Kubota et al., 1997); optimedin, also found in the vertebrate eye (Torrado et al., 2002); olfactomedin, a major protein in the extracellular matrix of the olfactory epithelium (Snyder et al., 1991); tiarin, a dorsalizing factor in *Xenopus* embryos (Tsuda et al., 2002); and amassin, a secreted protein responsible for clotting of coelomocytes in the sea urchin (Hillier and Vacquier, 2003).

The olfactomedin domain is responsible for formation of oligomers of olfactomedin (Snyder et al., 1991) and of amassin (Hillier and Vacquier, 2003). However, olfactomedin-related proteins associate by other means as well. In MYOC, homoprotein interaction occurs via the more N-terminal leucine zipper domain (Fautsch and Johnson, 2001), but the olfactomedin domain is necessary for proper protein folding and secretion, as well as interaction with other proteins (Caballero and Borras, 2001; Caballero et al., 2000; Gobeil et al., 2004). Our results demonstrate that Noelins-1 and -4 interact biochemically even though Noelin-4 does not contain an olfactomedin domain. This interaction may occur through disulfide bridges between the two conserved cysteine residues in the M region. These residues are homologous to cysteine residues found in olfactomedin, MYOC, tiarin and amassin, and are outside of the olfactomedin domain in all of these proteins (see Hillier and Vacquier, 2003).

An intriguing analogy to our findings regarding the interaction between Noelin-1 and Noelin-4 exists in the vertebrate eye. MYOC, which is mutated in some forms of primary open angle glaucoma, interacts with optimedin in co-immunoprecipitation assays. In transfected cells, mutant MYOC interferes with secretion of optimedin, causing it to be sequestered in the endoplasmic reticulum (Torrado et al., 2002). These results are significant because they provide another example of olfactomedin-related proteins binding to each other in a manner that affects each other's function. In the present case, over-expression of *Noelin-4* causes over-growth of the neural plate territory leading to several mispatterning anomalies in the later embryo. However, co-expression of Noelin-1, which binds to Noelin-4, strongly reduces this activity.

The ability of Noelin-1 and -4 to bind does not rule out the possibility that Noelins may interact with other proteins. Good candidates for such an interaction are other olfactomedin-domain proteins. Strikingly, *Xenopus tiarin* is expressed in tissues adjacent to *Noelin*-expressing tissues during early development (Moreno and Bronner-Fraser, 2001; Tsuda et al., 2002). *Tiarin* over-expression causes a dorsalized phenotype, with expansion of dorsal markers in the neural tube and loss of ventral marker expression, while *Noelin-4* over-expression causes expansion of the neural territory. One possibility is that these two proteins may interact in vivo such that *Noelin-4* potentiates the function of *tiarin*. The emerging hypothesis is that interaction of olfactomedin-domain proteins may result in modifications of their cellular localization and function.

Our data uncover a novel role for Noelins in balancing the timing of neuronal differentiation. Several lines of evidence support the possibility that interactions between Noelins may influence this timing. First, *Noelin-1* over-expression in neuralized animal caps promotes neuronal differentiation at an earlier stage (Moreno and Bronner-Fraser, 2001). Second, *Noelin-4* neural expansion activity is often accompanied by a delay in expression of the neuronal differentiation marker, *N-tubulin*. Third, *Noelin-1* rescues the neural precursor expansion phenotype of *Noelin-4*. Certainly, the picture is more complicated than these two factors alone determining the timing of differentiation. *Noelin* expression is robust only after neurons become postmitotic, and in fact are induced by neurogenic genes like X*NeuroD* and *X-ngnr-1*. Additionally, in gain-of-function experiments, *Noelins* act downstream of early inductive events; for example, *Noelin-1* only promotes premature neuronal differentiation in neuralized animal caps, but not in whole embryos. Similarly, *Noelin-4* can alter neural precursor fate only in tissues contiguous with endogenous neural tissue, suggesting that it promotes this fate in non-neural tissue that may have been exposed to neuralizing signals rather than acting as an inducer itself. In this regard, it does not induce neural fate in ventral ectoderm. This implies that Noelins require other cofactors or certain cellular contexts to exert these functions. In cells that

endogenously express Noelins, differential regulation of Noelin isoform levels or activity may result in modulation of neural precursors between undifferentiated and differentiated states.

Note added in proof

A recent publication by Ando and colleagues investigated the biochemistry of mouse Pancortin-3 (*Noelin-2*) and presents results consistent with our findings in Xenopus. On Western blots, they find evidence that all four Pancortins multimerize, and show specifically that Pancortin-3 forms oligomers. In addition, the two conserved cysteine residues in the common M region were found to be necessary for multimerization and secretion of Pancortin-3 (Ando et al., 2005).

Acknowledgments

We are grateful to Drs. Clare Baker, Laura Gammill, Anne Knecht and Carole LaBonne for critical reading of the manuscript and helpful discussions during the course of this work. We thank Johanna Tan who provided excellent technical assistance. cDNA libraries and constructs used were kind gifts of R. Harland, M. King, and Y. Sasai. T.A.M. was a fellow of the ARCS foundation. This work was supported by NIH grant NS42287 to M.B.-F.

References

Altschul, S.F., Gish, W., Miller, W., Myers, E.W., Lipman, D.J., 1990. Basic local alignment search tool. J. Mol. Biol. 215, 403–410.

Ando, K., Nagano, T., Nakamura, A., Konno, D., Yagi, H., Sato, M., 2005. Expression and characterization of disulfide bond use of oligomerized A2-Pancortins: extracellular matrix constituents in the developing brain. Neuroscience 133, 947–957.

Barembaum, M., Moreno, T.A., LaBonne, C., Sechrist, J., Bronner-Fraser, M., 2000. Noelin-1 is a secreted glycoprotein involved in generation of the neural crest. Nat. Cell Biol. 2, 219–225.

Brunet, J.F., Ghysen, A., 1999. Deconstructing cell determination: proneural genes and neuronal identity. Bioessays 21, 313–318.

Caballero, M., Borras, T., 2001. Inefficient processing of an olfactomedin-deficient myocilin mutant: potential physiological relevance to glaucoma. Biochem. Biophys. Res. Commun. 282, 662–670.

Caballero, M., Rowlette, L.L., Borras, T., 2000. Altered secretion of a TIGR/MYOC mutant lacking the olfactomedin domain. Biochim. Biophys. Acta 1502, 447–460.

Chang, C., Hemmati-Brivanlou, A., 1998. Cell fate determination in embryonic ectoderm. J. Neurobiol. 36, 128–151.

Danielson, P.E., Forss-Petter, S., Battenberg, E.L., deLecea, L., Bloom, F.E., Sutcliffe, J.G., 1994. Four structurally distinct neuron-specific olfactomedin-related glycoproteins produced by differential promoter utilization and alternative mRNA splicing from a single gene. J. Neurosci. Res. 38, 468–478.

Fautsch, M.P., Johnson, D.H., 2001. Characterization of myocilin–myocilin interactions. Invest. Ophthalmol. Visual Sci. 42, 2324–2331.

Ferreiro, B., Kintner, C., Zimmerman, K., Anderson, D., Harris, W.A., 1994. XASH genes promote neurogenesis in *Xenopus* embryos. Development 120, 3649–3655.

Gobeil, S., Rodrigue, M.A., Moisan, S., Nguyen, T.D., Polansky, J.R., Morissette, J., Raymond, V., 2004. Intracellular sequestration of hetero-oligomers formed by wild-type and glaucoma-causing myocilin mutants. Invest. Ophthalmol. Visual Sci. 45, 3560–3567.

Harland, R., 2000. Neural induction. Curr. Opin. Genet. Dev. 10, 357–362.

Hemmati-Brivanlou, A., de la Torre, J.R., Holt, C., Harland, R.M., 1991. Cephalic expression and molecular characterization of *Xenopus* En-2. Development 111, 715–724.

Hillier, B.J., Vacquier, V.D., 2003. Amassin, an olfactomedin protein, mediates the massive intercellular adhesion of sea urchin coelomocytes. J. Cell Biol. 160, 597–604.

Hopwood, N.D., Pluck, A., Gurdon, J.B., 1989. A *Xenopus* mRNA related to *Drosophila* twist is expressed in response to induction in the mesoderm and the neural crest. Cell 59, 893–903.

Knecht, A.K., Good, P.J., Dawid, I.B., Harland, R.M., 1995. Dorsal-ventral patterning and differentiation of noggin-induced neural tissue in the absence of mesoderm. Development 121, 1927–1935.

Kondo, D., Yamamoto, T., Yaoita, E., Danielson, P.E., Kobayashi, H., Ohshiro, K., Funaki, H., Koyama, Y., Fujinaka, H., Kawasaki, K., Sutcliffe, J.G., Arakawa, M., Kihara, I., 2000. Localization of olfactomedin-related glycoprotein isoform (BMZ) in the Golgi apparatus of glomerular podocytes in rat kidneys. J. Am. Soc. Nephrol. 11, 803–813.

Kroll, K.L., Salic, A.N., Evans, L.M., Kirschner, M.W., 1998. Geminin, a neuralizing molecule that demarcates the future neural plate at the onset of gastrulation. Development 125, 3247–3258.

Kubota, R., Noda, S., Wang, Y., Minoshima, S., Asakawa, S., Kudoh, J., Mashima, Y., Oguchi, Y., Shimizu, N., 1997. A novel myosin-like protein (myocilin) expressed in the connecting cilium of the photoreceptor: molecular cloning, tissue expression, and chromosomal mapping. Genomics 41, 360–369.

Kulkarni, N.H., Karavanich, C.A., Atchley, W.R., Anholt, R.R., 2000. Characterization and differential expression of a human gene family of olfactomedin-related proteins. Genet. Res. 76, 41–50.

Lee, J.E., Hollenberg, S.M., Snider, L., Turner, D.L., Lipnick, N., Weintraub, H., 1995a. Conversion of *Xenopus* ectoderm into neurons by NeuroD, a basic helix–loop–helix protein. Science 268, 836–844.

Lee, J.E., Hollenberg, S.M., Snider, L., Turner, D.L., Lipnick, N., Weintraub, H., 1995b. Conversion of *Xenopus* ectoderm into neurons by NeuroD, a basic helix–loop–helix protein. Science 268, 836–844.

Ma, Q., Kintner, C., Anderson, D.J., 1996. Identification of neurogenin, a vertebrate neuronal determination gene. Cell 87, 43–52.

Mayor, R., Morgan, R., Sargent, M.G., 1995. Induction of the prospective neural crest of *Xenopus*. Development 121, 767–777.

Mizuseki, K., Kishi, M., Matsui, M., Nakanishi, S., Sasai, Y., 1998a. *Xenopus* Zic-related-1 and Sox-2, two factors induced by chordin, have distinct activities in the initiation of neural induction. Development 125, 579–587.

Mizuseki, K., Kishi, M., Shiota, K., Nakanishi, S., Sasai, Y., 1998b. SoxD: an essential mediator of induction of anterior neural tissues in *Xenopus* embryos. Neuron 21, 77–85.

Moreno, T.A., Bronner-Fraser, M., 2001. The secreted glycoprotein Noelin-1 promotes neurogenesis in *Xenopus*. Dev. Biol. 240, 340–360.

Moreno, T.A., Bronner-Fraser, M., 2002. Neural expression of mouse Noelin-1/2 and comparison with other vertebrates. Mech. Dev. 119, 121.

Munro, S., Pelham, H.R., 1987. A C-terminal signal prevents secretion of luminal ER proteins. Cell 48, 899–907.

Nagano, T., Nakamura, A., Mori, Y., Maeda, M., Takami, T., Shiosaka, S., Takagi, H., Sato, M., 1998. Differentially expressed olfactomedin-related glycoproteins (Pancortins) in the brain. Mol. Brain Res. 53, 13–23.

Nagano, T., Nakamura, A., Konno, D., Kurata, M., Yagi, H., Sato, M., 2000. A2-Pancortins (Pancortin-3 and -4) are the dominant pancortins during neocortical development. J. Neurochem. 75, 1–8.

Nieuwkoop, P.D., Faber, J., 1967. Normal Table of *Xenopus laevis* (Daudin). North-Holland, Amsterdam.

Nielsen, H., Engelbrecht, J., Brunak, S., von Heijne, G., 1997. Identification of prokaryotic and eukaryotic signal peptides and prediction of their cleavage sites. Protein Eng. 10, 1–6.

Rupp, R.A., Snider, L., Weintraub, H., 1994. *Xenopus* embryos regulate the nuclear localization of XMyoD. Genes Dev. 8, 1311–1323.

Saka, Y., Smith, J.C., 2001. Spatial and temporal patterns of cell division during early *Xenopus* embryogenesis. Dev. Biol. 229, 307–318.

Sasai, Y., De Robertis, E.M., 1997. Ectodermal patterning in vertebrate embryos. Dev. Biol. 182, 5–20.

Sive, H.L., Grainger, R.M., Harland, R.M., 2000. Early Development of *Xenopus laevis*: A Laboratory Manual. Cold Spring Harbor Laboratory Press, Plainview, New York. 338 pp.

Slack, J.M., Forman, D., 1980. An interaction between dorsal and ventral regions of the marginal zone in early amphibian embryos. J. Embryol. Exp. Morphol. 56, 283–299.

Snyder, D.A., Rivers, A.M., Yokoe, H., Menco, B.P., Anholt, R.R., 1991. Olfactomedin: purification, characterization, and localization of a novel olfactory glycoprotein. Biochemistry 30, 9143–9153.

Torrado, M., Trivedi, R., Zinovieva, R., Karavanova, I., Tomarev, S.I., 2002. Optimedin: a novel olfactomedin-related protein that interacts with myocilin. Hum. Mol. Genet. 11, 1291–1301.

Tsuda, H., Sasai, N., Matsuo-Takasaki, M., Sakuragi, M., Murakami, Y., Sasai, Y., 2002. Dorsalization of the neural tube by *Xenopus tiarin*, a novel patterning factor secreted by the flanking nonneural head ectoderm. Neuron 33, 515–528.

Turner, D.L., Weintraub, H., 1994. Expression of achaete–scute homolog 3 in *Xenopus* embryos converts ectodermal cells to a neural fate. Genes Dev. 8, 1434–1447.

Weinstein, D.C., Hemmati-Brivanlou, A., 1999. Neural induction. Annu. Rev. Cell Dev. Biol. 15, 411–433.

Yokoe, H., Anholt, R.R., 1993. Molecular cloning of olfactomedin, an extracellular matrix protein specific to olfactory neuroepithelium. Proc. Natl. Acad. Sci. U. S. A. 90, 4655–4659.